NIH Public Access
Author Manuscript
*Chem Res Toxicol*. Author manuscript; available in PMC 2009 October 26.

Published in final edited form as:
*Chem Res Toxicol*. 2008 May ; 21(5): 1143–1153. doi:10.1021/tx700415b.

# Procainamide, but not *N*-Acetylprocainamide, Induces Protein Free Radical Formation on Myeloperoxidase: A Potential Mechanism of Agranulocytosis

**Arno G. Siraki**[*,§], **Leesa J. Deterding**[#], **Marcelo G. Bonini**[*], **JinJie Jiang**[*], **Marilyn Ehrenshaft**[*], **Kenneth B. Tomer**[#], and **Ronald P. Mason**[*]

[*]Laboratory of Pharmacology and Chemistry, National Institute of Environmental Health Sciences, National Institutes of Health, 111 Alexander Dr., Research Triangle Park, NC USA, 27709.

[#]Laboratory of Structural Biology, National Institute of Environmental Health Sciences, National Institutes of Health, 111 Alexander Dr., Research Triangle Park, NC USA, 27709.

## Abstract

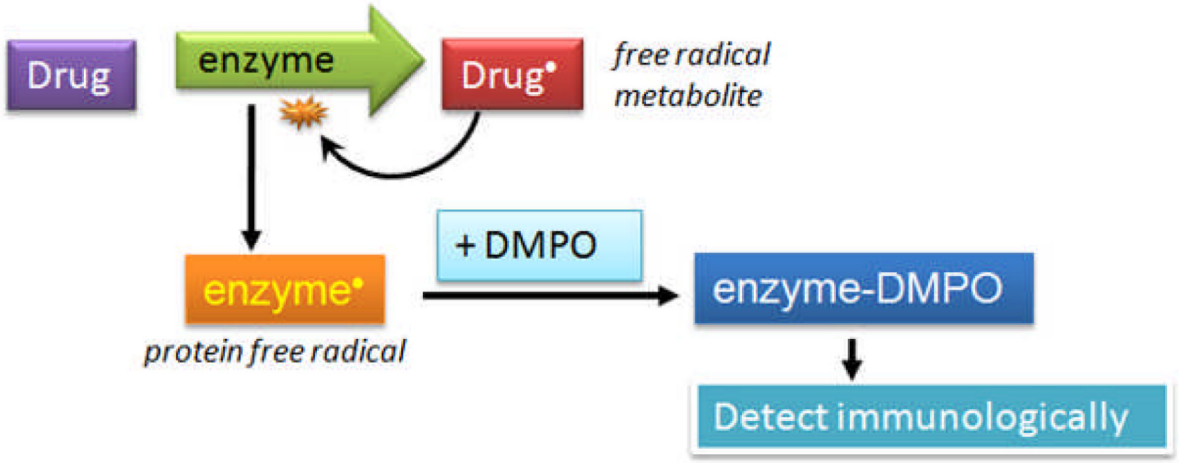


Procainamide (PA) is a drug that is used to treat tachycardia in post-operative patients or for long term maintenance of cardiac arrythmias. Unfortunately, its use has also been associated with agranulocytosis. Here we have investigated the metabolism of PA by myeloperoxidase (MPO) and the formation of an MPO protein free radical. We hypothesized that PA oxidation by MPO/$H_2O_2$ would produce a PA cation radical that, in the absence of a biochemical reductant, would lead to the free-radical oxidation of MPO. We utilized a novel anti-DMPO antibody to detect DMPO (5,5-dimethyl-1-pyrroline *N*-oxide) covalently bound to protein, which forms only by the reaction of DMPO with a protein free radical. We found that PA metabolism by MPO/$H_2O_2$ induced the formation of DMPO-MPO, which was inhibited by MPO inhibitors and ascorbate. *N*-acetyl-PA did not cause DMPO-MPO formation, indicating that the unsubstituted aromatic amine was more oxidizable. PA had a lower calculated ionization potential than *N*-acetyl-PA. The DMPO adducts of

§To whom correspondence should be addressed: Laboratory of Pharmacology and Chemistry, National Institute of Environmental Health Sciences, 111 TW Alexander Dr., Research Triangle Park, NC USA, 27709. T: (919) 541-5197, F: (919) 541-1043, sirakia@niehs.nih.gov..

Abbreviations: PA, procainamide; NAPA, *N*-acetyl-procainamide; MPO, myeloperoxidase; ESR, electron spin resonance; DTPA, diethylenetriaminepentaacetic acid; MNP, 2-methyl-2-nitrosopropane; DMPO, 5,5-dimethyl-1-pyrroline *N*-oxide; ABAH, 4-aminobenzoic acid hydrazide; G/GO,Glucose / glucose oxidase.

MPO metabolism, as analyzed by electron spin resonance spectroscopy, included a nitrogen-centered radical and a phenyl radical derived from PA, either of which may be involved in the free radical formation on MPO. Furthermore, we also found protein-DMPO adducts in MPO-containing, intact human promyelocytic leukemia cells (HL-60). MPO was affinity-purified from HL-60 cells treated with PA/$H_2O_2$ and was found to contain DMPO using the anti-DMPO antibody. Mass spectrometry analysis confirmed the identity of the protein as human MPO. These findings were also supported by the detection of protein free radicals with electron spin resonance in the cellular cytosolic lysate. The formation of an MPO protein free radical is believed to be mediated by free radical metabolites of PA, which we characterized by spin trapping. We propose that drug-induced free radical formation on MPO may play a role in the origin of agranulocytosis.

Procainamide (PA) is a sodium channel blocker which stabilizes electrical conduction in the heart. It is used for treating atrial tachycardia and is specifically recommended for atrial fibrillation of the Wolff-Parkinson-White syndrome (1). Unfortunately, agranulocytosis, an idiosyncratic adverse drug reaction, is associated with the use of procainamide (PA). This condition is characterized by severe neutropenia, where the absolute neutrophil count decreases below 500/uL (2,3), which greatly increases the risk of bacterial infection. Septic complications have been documented in a number of case reports (4-6): A study in the Netherlands between 1974-1994 revealed a 1 % incidence of PA-induced agranulocytosis (7), and another study reported 0.5 – 4% (8). The annual risk of agranulocytosis to the general population has been reported as 3.4 per million with greater than two-thirds of all cases are attributed to pharmaceutical drug use (9,10). The mechanism of drug-induced agranulocytosis, however, is unknown, and there is no suitable screening assay for it in drug development. As agranulocytosis is an unpredictable event during the course of drug therapy, any insight into the mechanism of drug-induced agranulocytosis would be significant.

It has been proposed that neutrophil myeloperoxidase (MPO) activates xenobiotics to reactive intermediates that mediate further events to produce an adverse drug reaction (11). Arylamine drugs have been proposed to form *N*-hydroxylamine metabolites catalyzed by mixed function oxidases that lead to nitroso metabolites (11,12), which are proposed to bind covalently to proteins that may be involved in agranulocytosis. However, such a free radical metabolite-mediating protein radical formation has not previously been considered or evaluated.

The mature neutrophil is estimated to contain ~5% myeloperoxidase stored within azurophilic cytosolic granules (13). HL-60 cells derived from a patient with acute promyelocytic leukemia also contain similar amounts of MPO. Although the primary role of MPO is considered to be the formation of bactericidal hypochlorous acid from chloride and $H_2O_2$, this enzyme behaves similarly to other peroxidases in its metabolism of many organic xenobiotics, including phenols and anilines (14,15).

Native MPO is comprised of two heavy (~59 kDa) and two light (~14 kDa) polypeptide subunits with a weight of ~150 kDa (16). Each heavy-light set (referred to as hemi-MPO) contains catalytic activity just as the native enzyme does (17). Each hemi-MPO (~78 kDa) is linked via one disulfide bond, and the heavy and light subunits are also linked by one disulfide bond, making a total of three disulfide bonds per native enzyme. One heme active site is located in each heavy subunit, giving two heme active sites per native MPO (18).

PA is an aniline derivative and is most likely a peroxidase substrate (14,19). A previous study found indirect evidence of PA free radical metabolites by measuring NADH oxidation (20); however, the radical metabolites were not characterized. The first product of PA metabolism by MPO/$H_2O_2$ would presumably be a nitrogen-centered cation radical, which we show decomposes into a *para*-substituted phenyl radical. We hypothesize that one or both of these species attack MPO to form a protein free radical. We have elaborated this concept previously

using aminoglutethimide, another aniline-based drug (21). Since an immune response has been associated with certain instances of drug-induced agranulocytosis, it is possible that protein free radicals may trigger an autoimmune response against MPO or other neutrophil proteins. For example, propylthiouracil, an anti-thyroid drug that has a risk of agranulocytosis, has been shown to result in the formation of anti-MPO antibodies in patients (22) and in cats (23).

Herein, we show that PA induced the formation of a protein free radical on MPO, and demonstrate the detection of protein-DMPO adducts from intact HL-60 cells. We have also identified a PA free radical metabolite produced from MPO/$H_2O_2$ metabolism that we believe mediated the protein radical formation on MPO.

## Experimental Procedures

### Chemicals

Human MPO and 4-aminobenzoic acid hydrazide (ABAH) were purchased from Calbiochem (San Diego, CA). MPO was dissolved in 0.1 M phosphate buffer, pH 7.4, and dialyzed overnight against the same buffer with Slide-A-Lyzer® dialysis cassettes (10,000 MWCO; Pierce Biotechnology, Rockford, IL). Its concentration was determined by its extinction coefficient of 178 $mM^{-1}cm^{-1}$ at 429 nm (24). PA hydrochloride (Sigma-Aldrich, St. Louis, MO) was dissolved in NaOH at pH 11 and extracted into chloroform, which was evaporated. The resulting PA oil was assayed against PA standard to determine the concentration. *N*-acetyl-PA (NAPA), diethylenetriaminepentaacetic acid (DTPA), methyl α-D-mannopyranoside, concanavalin A, and 2-methyl-2-nitrosopropane (MNP) were purchased from Sigma Chemical Co. (St. Louis, MO). The latter was dissolved in buffer (3 mg/mL), covered in foil, sealed, and shaken overnight at 32 °C. 5,5-Dimethyl-1-pyrroline *N*-oxide (DMPO) was purchased from Alexis Biochemicals (San Diego, CA), purified twice by vacuum distillation at room temperature, and stored under argon atmosphere at -80 °C until use. Hydrogen peroxide (30% v/v, $H_2O_2$) was obtained from Fisher Scientific Co. (Fair Lawn, NJ) and was assayed by its extinction coefficient of 43.6 $M^{-1}cm^{-1}$ at 240 nm (25). Chelex-100 resin was purchased from Bio-Rad Laboratories (Hercules, CA).

### Spectrophotometry

Spectrophotometry was performed with a Cary 100 spectrophotometer (Varian Inc., CA) using a 500 μL quartz cuvette. Reactions were carried out in 0.1 M phosphate buffer (Chelex-100 treated with 100 μM DTPA), pH 7.4. The spectrophotometer was set to kinetic scan mode, where each scan was recorded every minute for 60 minutes. The scan rate was set at 600 nm/min between 400 and 500 nm to measure the MPO Soret spectrum. The baseline was derived from the buffer alone. MPO (500 nM) was added first, followed by PA and/or $H_2O_2$. MPO peroxidase activity was also determined after treatment of 50 nM MPO with 10-1000 μM PA / 100 μM $H_2O_2$ for 60 minutes. This solution was centrifuged with Microcon 50,000 MW cut-off centrifugal filters (Millipore) and resuspended in 0.1 M phosphate buffer pH 7.4, after which 5 mM guaiacol and 100 μM $H_2O_2$ (final concentration) were added. The formation of the guaiacol tetramer ($\lambda$ = 470 nm) was used as a measure of peroxidase activity (26).

### Enzyme-linked immunosorbent assay (ELISA)

ELISA plates (96-well, Greiner Labortechnik, Germany) were used to carry out the reaction and to detect the DMPO-MPO adduct. Optimal concentrations were determined by varying the concentration of AG, $H_2O_2$, DMPO, and MPO one at a time (data not shown).These reactions were carried out as described previously (21).

### Electron spin resonance (ESR)

A PA free radical metabolite was detected by spin trapping (27), where the free radical metabolite covalently binds to the nitroso spin trap (MNP) to produce a relatively stable nitroxide adduct. ESR spectra were obtained with a Bruker EMX spectrometer (Billerica, MA) equipped with an ER 4122 SHQ cavity operating at 9.78 GHz and 100 KHz modulation field at room temperature with the following parameters: power = 20 mW, scan rate = 0.47 G/s, modulation amplitude = 0.4 G, and receiver gain = $6.32\times10^5$. Spectra were recorded at four scans per reaction (355 s/scan, time constant = 327 ms). Spectra were simulated using WinSim v1.0 software (http://epr.niehs.nih.gov/) running on a desktop PC. For protein free radical detection, we employed conditions described previously (21).

### Cell culture and treatment

HL-60 cells were maintained as described previously (21) in RPMI-1640 medium (Invitrogen, Gibco #11875119) containing 10% FBS, 31 μg/mL penicillin, 50 μg/mL streptomycin, 10 μL/mL fungizone, 27 mM $NaHCO_3$, 16 mM HEPES, and 8 mM MOPS in a water-jacketed incubator. Cells were centrifuged, washed once, resuspended in RPMI-1640 (no serum) to a concentration of $2 \times 10^6$ cells/mL, and plated in 12-well plates (Corning Inc., Corning, NY) for experiments. DMPO (50 mM) was added 10 minutes prior to adding 5 mM glucose and 50 mU/mL glucose oxidase, which initiated the reaction. This concentration initially produced 5 μM $H_2O_2$ per minute, but required mixing since the reaction is oxygen-dependent. Thirty minutes prior to initiating the reaction, either ABAH (1 mM) or azide (2 mM), together with 100 μM $H_2O_2$, was added. The cell suspensions containing ABAH or azide (as well as those with no inhibitors) were washed and replaced with fresh media before the reaction. Ascorbate or dehydroascorbate was added 30 minutes before PA; PA and NAPA were added 1 minute before initiating the reaction At the desired timepoints, the cells were centrifuged at 50 × g for 5 minutes to remove the supernatant and washed twice. Cell viability was assessed measuring relative ATP levels using Cell-Titer Glo® Cell Viability Assay (Promega Corp., Madison, WI). The remaining cells were lysed with RIPA buffer (0.05 g sodium deoxycholate, 100 μL Triton X-100, 10 μL of 10% SDS, in 10 mL of 0.1 M PBS) containing protease inhibitors (Complete, Mini Protease Inhibitor Cocktail Tablets, Roche Applied Science, IN). After 30 minutes, the samples were centrifuged at 20,000 × g for 20 minutes. The soluble material (supernatant) was stored at 4 °C until use for Western blots.

### Western blot

Western blots were run under reducing conditions, and were performed as described previously with minor changes (21,28). Membranes that were stripped using Restore™ PLUS Western Blot Stripping Buffer (Pierce) were first probed with anti-DMPO before stripping (60 min with mixing). Membranes were blocked for 30 min and reprobed with anti-MPO.

### Affinity purification of MPO from HL-60 cells

Affinity purification was performed after treatment of the HL-60 cells with DMPO, glucose/glucose oxidase, and drugs. A volume of 5 mL of cells was used to ensure an adequate yield of MPO. We followed the method of Hope *et al*., which is based on using concanavalin A to bind MPO (which is glycosylated) and separate it out from the protein mixture (29). These procedures were carried out as described previsouly (21).

### Calculation of Energy of the Ionization Potential

The structures of PA and NAPA were sketched in Sybyl 7.3 (Tripos, Inc.). Structures were energy minimized according to the Powell method with the following parameters: force field = Tripos, charges = Gasteiger-Huckel, dielectric constant = 80 (water). After energy minimization, MOPAC v.6 was used to calculate the ionization potential using AM1

parameters. The same calculations were performed with PM3 parameters for validation of results.

### Mass Spectrometry

The protein band(s) was manually excised from the gel, cut into small pieces, and transferred into a 96-well microtiter plate. Gel pieces were subjected to automatic tryptic digestion using a method similar to that described previously (30). For the nanoLC/ESI/MS/MS analyses, an Agilent XCT Ultra ion trap (Agilent Technologies, Inc., Santa Clara, CA) equipped with an HPLC-Chip Cube MS interface and an Agilent 1100 nanoLC system was used. Injections of 30 μL from the peptide digests were made onto a 40 nL enrichment column followed by a 43 mm × 75 μm analytical column, packed with ZORBAX 300SB C18 particles. Peptides were separated and eluted using a linear gradient of 3-50% acetonitrile (0.1% formic acid) over 40 min, followed by a linear gradient of 50-95% acetonitrile over 7 min at a flow rate of 500 nL/min. The ion trap mass spectrometer settings were as follows: positive ion, standard enhanced mode; capillary voltage, -2150 V; mass range, 300-1500; ICC smart target (number of ions in the trap prior to scan out), 100,000 or 200 milliseconds of accumulation; and MS/MS fragmentation amplitude, 1.0 V. During the LC/MS/MS analyses, automated data-dependent acquisition software was employed with the six most abundant ions (threshold requirement of 10,000 counts) from each spectrum selected for MS/MS analysis.

Following the analyses, the MS/MS data were extracted and analyzed using Spectrum Mill MS Proteomics software (Agilent Technologies, Inc). To generate peak lists, the raw data files were processed using the Data Extractor function with the following parameters: deconvoluted ions of 300-6,000 Da and a retention time of 10 to 60 min. MS scans with the same precursor m/z were merged based on a +/- 1.4 m/z window and a +/- 15 sec retention time window. Using the extracted data, searches were performed against the NCBI nonredundant protein database using the MS/MS search function.

## Results

### Ionization Potential of PA and NAPA

The ionization potentials of PA and NAPA were calculated using the MOPAC interface in Sybyl 7.3, and the results are shown in Table 1. NAPA has a calculated ionization potential of 9.05 eV, and the ionization potential of PA was 8.70 eV according the AM1 geometry. We repeated the energy calculations using PM3 parameters and found that NAPA ionization potential was 8.97 eV and PA was 8.43 eV. These data confirm that more energy is required to oxidize NAPA than PA.

### MPO Compound II accumulation occurs in the presence of PA/$H_2O_2$

Anti-inflammatory drugs have been shown to accumulate MPO in Compound II form. This form of the enzyme is unable to catalyze hypochlorous acid formation, which appears to be characteristic of poor peroxidase substrates (19). As shown in Fig. 1A, when 80 μM $H_2O_2$ was added to 500 nM MPO, there was a rapid formation of Compound II (λ = 455 nm), followed by a gradual return to the resting enzyme (λ = 429 nm). Although Compound I is initially formed, it cannot be detected in conventional spectrophotometry because of its rapid reduction to Compound II (31). However, in the presence of 20 μM PA and 80 μM $H_2O_2$ (Fig. 1B), MPO Compound II reduction was delayed, but did begin to return to the resting state. It appears that PA belongs to a class of substrates that are good substrates for Compound I, but poor substrates for Compound II (19). Such substrates have been shown to inhibit $Cl^-$ oxidation, which is carried out only by MPO Compound I. Incubation of PA (10 – 1,000 μM) with MPO/$H_2O_2$ for 1 hour did not result in irreversible inhibition of peroxidase activity as assayed by guaiacol tetramer formation (data not shown).

### ESR spectra of a PA-derived phenyl radical metabolite with MNP

PA reacted with MPO/$H_2O_2$ in the presence of MNP to produce an ESR spectrum consisting of 21 lines arranged in three sets of seven lines (Fig. 2A). Controls without PA (Fig. 2C) or without MPO (Fig. 2D) failed to form this radical adduct. When MPO was incubated with 250 μM ABAH/250 μM $H_2O_2$ (E) or 500 μM azide/500 μM $H_2O_2$ (F) for 30 minutes prior to the addition of PA, MNP, and 1 mM $H_2O_2$, the spectrum was completely inhibited. Incubation of MPO with 500 μM $H_2O_2$ for 30 minutes resulted in no inhibition of activity (data not shown).

The spectrum formed in the complete system, characteristic of a small, rapidly rotating free radical, is predominantly the spectrum of an MNP radical adduct of a PA-derived radical. Computer simulation of this spectrum produced a close match (r = 0.995) to the experimental spectrum in A (Fig. 2B). This simulated spectrum consisted of one species, which contained two hydrogen hyperfine splitting constants ($a^H$ = 1.98 G and $a^H$ = 0.97 G) each from two equivalent hydrogens ($a^H_{(3)} = a^H_{(5)}$ = 1.98 G; $a^H_{(2)} = a^H_{(6)}$ = 0.97 G) and a nitroxide nitrogen ($a^N$ = 13.8 G). This species represents the radical adduct formed by the PA-derived phenyl radical metabolite reacting with MNP as proposed in Scheme 2. A large class of *t*-butyl-*para*-phenyl nitroxide radicals, which have been detected in water, have two equivalent hyperfine couplings of about 2 G arising from two ortho hydrogens and two equivalent hyperfine coupling constants of about 1 G arising from the two meta hydrogens (32-35). The structure of this phenyl radical metabolite is unambiguous. The presence of chloride did not attenuate this reaction (data not shown).

### ESR spectra of two PA-derived radical metabolites using DMPO

PA (5 mM) metabolism by 750 nM MPO / 1 mM $H_2O_2$ in the presence of 100 mM DMPO resulted in the formation of two radical adducts as shown in Figure 3A. When the DMPO concentration was reduced to 30 mM (Fig. 3E), less of the minor species was detected, and when 10 mM DMPO was used (Fig. 3F), the minor species was not detected. This implies that a primary species was trapped by the higher concentration of DMPO which gave rise to the minor radical adduct; the latter adduct is apparently more unstable that the other species. Both species were computer simulated (Fig. 3B) in a composite spectrum and closely matched (r = 0.99) the experimental spectrum. The coupling constants for species 1 (Fig. 3C, $a^N$ = 15.84 G and $a^H$ = 24.80 G) with its rather high β-hydrogen coupling indicated that this species was derived from a DMPO-phenyl radical adduct (36). The smaller spectrum from species 2 (Fig. 3D, $a^N_{(nitroxide)}$ = 15.72 G, $a^N$ = 2.450 G, and $a^H$ = 18.22 G) was derived from a DMPO nitrogen-centered radical (37). This signal was not detectable when 10 mM DMPO was used (Fig. 3F), whereas the secondary phenyl radical adduct was detected. Typically, carbon-centered radical adducts of DMPO are more stable than nitrogen-centered radical adducts because the stronger carbon-carbon bond is formed by spin trapping the phenyl radical.

In Fig. 4, the complete system (Fig. 4A) contained the same reaction mixture as that in Fig. 3A. The inhibition of MPO was accomplished by incubating ABAH (Fig. 4B) or azide (Fig. 4C) with equimolar amounts of $H_2O_2$ with MPO for 30 minutes prior to the addition of PA, and similar to Fig. 2, the ESR signal of the complete system was inhibited. The incubation of 500 μM $H_2O_2$ alone with MPO did not result in any inhibition of enzyme activity (data not shown). The inclusion of 10 mM ascorbate in the complete system resulted in the detection of the ascorbyl radical (Fig. 4D). When NAPA was substituted for PA, the signal was attenuated (Fig. 4E). The absence of PA (Fig. 4F), MPO (Fig. 4G), or MPO and $H_2O_2$ resulted in a greatly attenuated signal. The signal found in Fig. 4G was abolished when 1 mM DTPA was included in the reaction, indicating that the spectrum was catalyzed by trace-metal contamination.

### ELISA detection of DMPO-MPO adducts and the effect of a PA congener, MPO inhibitors, and ascorbate

To test the involvement of the metabolic activation of PA in the formation of MPO protein free radicals, we used an ELISA and probed for DMPO-MPO using a polyclonal DMPO antibody developed in our laboratory (30). A significant signal was detected in the reaction system that contained DMPO, PA, $H_2O_2$, and MPO (Fig. 5). The absence of PA resulted in a 100-fold loss of luminescence. Formation of the DMPO-MPO adduct was inhibited by the prior presence of the MPO inhibitors ABAH and azide and by the antioxidant ascorbate. If these inhibitors were added after completion of the reaction, the signal was not affected (data not shown). When NAPA, the *N*-acetylated derivative of PA (shown in the inset), was substituted for PA, there was no significant increase in DMPO-MPO, and the luminescence was comparable to having no PA present. DMPO-MPO formation depended on PA concentration (inset); a biphasic pattern is apparent, with the optimum concentration of PA in this system reached at 100 μM. The presence of chloride in these reactions had no effect (data not shown).

### Western blot detection of anti-DMPO from intact HL-60 cells

To investigate production of protein-DMPO adducts in intact HL-60 cells, we incubated $2 \times 10^6$ cells/mL in serum free RPMI-1640 with DMPO, PA and glucose/glucose oxidase (to generate $H_2O_2$) for 4 h. As shown in Fig. 6A, this treatment produced band-specific anti-DMPO staining. Molecular weight markers showed the darkest anti-DMPO staining to occur on a protein between 50-75 kDa. Anti-MPO staining of the same samples showed that the heavy chain of MPO co-migrated with the anti-DMPO cross-reacting band and that each lane contained approximately the same amount of MPO (anti-MPO, Fig. 6A). ABAH and azide and the absence of glucose/glucose oxidase reduced DMPO-protein formation. Substitution of NAPA for PA resulted in less DMPO-protein formation. ATP levels in cells at the timepoint showed non-significant differences between treatments (data not shown).

In a separate experiment, we compared the effect of dehydroascorbate to ascorbate in their ability to decrease anti-DMPO detection induced by PA (Fig. 6B). This was performed since we have previously shown that ascorbate itself decreased anti-DMPO detection induced by another aromatic amine drug (21). However, ascorbate itself is not taken up by HL-60 cells; rather, dehydroascorbate is taken up and reduced to ascorbate inside the cell (38). It appeared that dehydroascorbate was slightly more effective in attenuating anti-DMPO detection than ascorbate.

### Detection of DMPO-MPO from affinity purified MPO from HL-60 cells

Reactions were carried out as described above for Western blot analysis after affinity purification of MPO was carried out on HL-60 cells (Fig. 6C). Only the complete system containing DMPO, glucose/glucose oxidase, and PA produced immunoreactivity with anti-DMPO, demonstrating that DMPO was bound to the MPO heavy chain (~55kDa). This membrane was stripped and reprobed with anti-MPO, which showed that MPO was present in each lane in approximately equal amounts.

### Protein identification by mass spectrometry

The Coomassie blue stained protein band (corresponding to the anti-DMPO band observed by Western blot in Fig. 6C) was subjected to mass spectrometric analyses for protein identification. The band was excised from the gel, digested, and analyzed by LC/MS/MS. Following analyses, the raw data were extracted and searched against the NCBI nonredundant database (species: human and rodent). Using this methodology, the protein in band 1 was identified as human myeloperoxidase (gi:4557759) with a summed MS/MS search score of 325.63. From the LC/MS/MS analyses, twenty-three distinct tryptic peptides were observed,

resulting in 35% sequence coverage. All MS/MS sequence assignments used for the protein identification were manually validated. These results verify that the protein band is myeloperoxidase. No other protein with a summed MS/MS search score greater than 30 was identified from the database search. At this scoring threshold, the false positive rate is essentially 0% as determined by searching against a reversed sequence database.

### ESR spectra of a protein radical from HL-60 cytosolic lysate

To support the results of the immunological detection of a DMPO-MPO adduct as seen with the ELISAs and Western blots, we recorded ESR spectra using a dialyzed preparation of HL-60 cytosol. Reactions contained 7.1 mg/mL protein lysate, 1mM MNP to trap protein radicals, 5 and 10 mM PA, and 1 mM $H_2O_2$, which was added last to initiate the reaction. DMPO did not give useful spectra possibly because the concentration of MPO present oxidized the DMPO nitroxide spin adducts. Therefore, we chose MNP as a spin trap since, unlike DMPO, its nitroxide spin adducts are not oxidizable to nitrones. Figure 7 shows a PA dose-dependent increase in protein free radical intensity (Fig. 7AB). The broad-lined (partially anisotropic) spectra are indicative of slowly tumbling macromolecule radical adducts (39). The same spectrum was attenuated in the presence of ABAH, azide, and ascorbate (Fig. 7C, D, E). The absence of either $H_2O_2$ (Fig. 7F) or PA (Fig. 7G) resulted in no protein radical formation. The substitution of NAPA for PA resulted in less protein radical formation (Fig. 7H).

## Discussion

We have shown that PA metabolism catalyzed by MPO resulted in the formation of a protein free radical on MPO, which was then trapped by DMPO and subsequently identified by the anti-DMPO antibody. In general, aromatic amines are well-known substrates for peroxidases. Examination of the Soret region of peroxidases is a common method for analyzing their catalytic cycle. We found that PA caused the accumulation of MPO Compound II. Our previous study with aminoglutethimide, another aromatic amine drug, showed that it kept MPO in its Compound II state for at least 60 min (entire scan duration), whereas with PA, Compound II reduction back to the resting enzyme began after 28 min (Fig. 1). Kettle and Winterbourn (19) have previously shown that other aromatic amine drugs inhibited hypochlorous acid formation, which has been attributed to the accumulation of Compound II. It is likely that PA also fits into this category of poor peroxidase substrates, since good substrates would efficiently reduce Compound II back to the resting state.

PA has previously been shown to form an *N*-hydroxylamine and *N*-chloro-PA when oxidzed by activated neutrophils or MPO/$H_2O_2$, and MPO/$H_2O_2$/$Cl^-$, respectively (40,41). It was shown previously that approximately 20% of PA results in *N*-chloro-PA in the presence of MPO/$H_2O_2$/$Cl^-$ and PA at pH 6 (41). We did not observe any attenuation from chloride, however, either because our experiments were carried out at pH 7.4, where no *N*-chloro-PA was formed, or because PA inhibited HOCl formation as described above. In this study, we have shown the peroxidase metabolism of PA to a substituted-phenyl radical demonstrated by ESR using spin trapping. The phenyl structure of the MNP adduct is unambiguous (32-35). Previously, an almost identical spectrum was found with sulfanilamide after UV photolysis (33). This spectrum was assigned to 4-sulfamoylbenzene-*t*-butylnitroxide. We recently showed that a very similar spectrum was observed in a similar system using aminoglutethimide; its metabolism also resulted in the formation of a phenyl radical (21). Therefore, based on the ESR spectrum obtained and its analogy to sulfanilamide as well as aminoglutethimide, we conclude that the PA free radical adduct with DMPO or MNP results from the cleavage of the N-C bond of the aniline moiety, with subsequent trapping of the phenyl radical (Scheme 1). This phenyl radical metabolite may be responsible for the formation of an MPO protein free radical by hydrogen abstraction or, possibly, its addition across an amino acid double bond

(Scheme 2). However, we also detected a nitrogen-centered cation radical with DMPO which was not observed at lower DMPO concentrations. The trapping of a nitrogen-centered radical with MNP could form a nitrogen-nitrogen bond of lower stability than the nitrogen-carbon bond of the DMPO-phenyl radical adduct. This suggests that the cation radical is the first radical metabolite formed, as expected. In addition, the PA cation radical will be a strong oxidant with an oxidation potential of about 1.03 V (42). As such, it may oxidize one or more aromatic amino acid residues of MPO.

In this study, MPO-catalyzed PA metabolism was immunochemically found to produce a positive response to the anti-DMPO antibody. We recently showed that aminoglutethimide also exhibited this activity (21). PA is another example of drug oxidation by an MPO/$H_2O_2$ system that resulted in a DMPO-protein adduct, (Scheme 2) which we propose occurs by the following reactions (equations 1-5):

$$\text{MPO (native)} + H_2O_2 \rightarrow \text{MPO (Compound I)} + H_2O \quad (1)$$

$$\text{MPO (Compound I)} + \text{PA} \rightarrow \text{MPO (Compound II)} + \text{PA}^{\bullet +} \quad (2)$$

$$\text{PA}^{\bullet +} \rightarrow \text{PA–derived phenyl}^{\bullet} \quad (3)$$

$$\text{PA}^{\bullet +} \text{ (or PA–derived phenyl}^{\bullet}) + \text{MPO} \rightarrow \text{MPO}^{\bullet} + \text{PA (or desamino–PA)} \quad (4)$$

$$\text{MPO}^{\bullet} + \text{DMPO} \rightarrow \text{MPO–DMPO}^{\bullet} \rightarrow \text{MPO–DMPO (nitrone)} \quad (5)$$

Interestingly, MPO, which itself catalyzed the oxidation of the drug to a free radical, was also the target of the resulting free radical reactive drug metabolite. As mechanism-based inhibitors of peroxidases have been proposed to form reactive free radical intermediates that bind to the heme active site and inhibit enzyme activity (43-46), we assayed the remaining peroxidase activity after incubation with PA. However, we found no inhibition of MPO peroxidase activity after treatment with PA (data not shown). It is unlikely, therefore, that a heme adduct results; a free radical on the protein chain (amino acid radical) is more likely. The affinity purified MPO was deglycosylated and the DMPO was still attached (data not shown), ruling out the possibility of a glycosyl radical. The specific site of radical formation, however, still remains to be identified.

The inhibition of anti-DMPO detection when MPO inhibitors were included in the reaction suggests that MPO catalytic activity is necessary for MPO protein free radical formation. ABAH (45) and azide (46) are both inhibitors of MPO, and both attenuated DMPO-MPO adduct formation. Ascorbate is a substrate in that MPO/$H_2O_2$ can oxidize ascorbate, but perhaps more importantly, ascorbate can rapidly reduce many radical intermediates formed by peroxidases (47). However, ascorbate is not taken up by HL-60 cells (38) even though we previously showed that ascorbate attenuated anti-DMPO detection when incubated before the addition of drug (21). Dehydroascorbate is taken up by cells and reduced intracellularly to ascorbate. It is certain that ascorbate oxidation in the cell media resulted in sufficient amounts of dehydroascorbate, which when to be taken up by the cells, was then reduced to ascorbate.

It is probable that ascorbate inhibited DMPO-MPO nitrone formation due to its reduction of the PA free radical metabolites, which prevented a radical attack on MPO.

The involvement of PA radical metabolites in MPO radical formation was also proven with the use of NAPA, an *N*-acetylated metabolite of PA. Others have shown that activated neutrophils produced significantly fewer cytotoxic NAPA metabolites compared to PA (48). Also, it has previously been shown that *N*-acetylbenzidine is a poorer peroxidase substrate than benzidine (49). A free amine should thus have a lower oxidation potential than its corresponding *N*-acetylated derivative. Consistent with this trend, we found that treating HL-60 cells with NAPA resulted in less DMPO bound to protein than in cells treated with PA.

We have shown above that NAPA has a greater ionization potential than PA. Ionization potential has been shown to have a linear relationship with energy of the highest occupied molecular orbital (50), and Koopman's theorem states that the latter is equal to the first ionization potential. Ionization potential is also related linearly to the oxidation potential (51). It is likely that less protein-DMPO resulted from NAPA metabolism because of its unfavorable oxidation potential. The importance of oxidation potential was shown in a study that investigated horseradish peroxidase/$H_2O_2$-catalyzed binding of aromatic hydrocarbons to DNA, where above a certain ionization potential, no DNA binding was observed (52)

The biphasic nature of DMPO-MPO formation (Fig. 3, inset) could be a result of prooxidant behavior of PA at low concentrations, after which PA reaches a threshold concentration where it becomes an antioxidant (53,54). This biphasic effect was also found with aminoglutethimide, suggesting that it could be a general phenomenon.

A better characterized side effect of PA than agranulocytosis is lupus, since there are clear serological biomarkers (anti-nuclear antibodies) that are associated with this autoimmune disease. When the role of PA acetylation was evaluated in patients, those patients receiving NAPA did not develop lupus, nor were anti-nuclear antibodies detected in their serum (55). Hydralazine is a hydrazine-based, anti-hypertensive drug that has a high risk of lupus. A study showed that hydralazine-induced lupus occurred almost exclusively in slow acetylator phenotype individuals (56), suggesting that the free amine of the drug was responsible for induction of the side-effect. Unfortunately, PA-induced agranulocytosis has a serum profile resembling the asymptomatic patient, as opposed to PA induced lupus (57). This fact, combined with the lower incidence of agranulcytosis compared with lupus, makes it difficult to reach a conclusion regarding the effect of acetylation polymorphisms on PA-induced agranulocytosis.

HL-60 cells were used to investigate whether DMPO-protein adducts could be detected in intact cells because, similar to human neutrophils, HL-60 cells contain 47.5 μg MPO / $10^7$ cells (16). Neutrophils can be primed by many different agents, all which result in the association of the NADPH oxidase complex which produces $H_2O_2$ (58). We used glucose/glucose oxidase to generate $H_2O_2$, which simulates the respiratory burst in neutrophils or macrophages. The formation of $H_2O_2$ as a co-substrate fueled the oxidation of PA by MPO. The model we have used may illustrate a possible outcome of PA use under a condition of inflammation since neutrophils and macrophages both produce $H_2O_2$ during infection. Our study showed that both enzymatically and with HL-60 cells, NAPA resulted in less protein free radical formation than PA.

In addition to the immunological detection of protein-DMPO in HL-60 cells formed from PA metabolism, the ESR spectra of HL-60 cell cytosol unequivocally showed the presence of a protein free radical that was PA-dependent and attenuated in both systems with MPO inhibitors, further validating its immunological detection. However, these ESR experiments could not provide information regarding the identity of the protein target. The Western blot from HL-60 cell cytosol indicated a DMPO-containing band of between 50 and 75 kDa, which led us to

consider that the target may be the heavy chain of MPO whose molecular weight has been reported from 55 to 62 kDa (16,17,59,60). Through the use of concanavalin A, an affinity purification resin for glycoproteins, we were able to partially purify MPO from the HL-60 cells and detect DMPO binding induced by PA. Mass spectrometry of the corresponding Coomassie blue stained gel showed that this band was MPO.

We propose that the free radical metabolism of PA may be implicated in agranulocytosis. A case report of two patients under PA treatment showed that their serum IgG was immunoreactive against leukemia cell lines (HL-60 or K-652 cells), resulting in T-cell mediated cytotoxicity (61). There was approximately 2- to 4-fold more complement-induced lysis against HL-60 cells than K-562 cells. Interestingly, K-562 cells do not constitutively express MPO, in contrast to HL-60 cells (62).

We propose that free radical formation on MPO by PA free radical metabolites may be implicated in agranulocytosis. We propose that free radical modification of MPO or other neutrophil proteins *in vivo* may lead to anti-neutrophil antibody formation and granulocyte death via immune-mediated mechanisms. We believe that MPO free radicals are formed either by oxidation of the protein by a PA-derived free radical, or through covalent binding by a PA-derived free radical across a double bond. It should be pointed out that PA-derived electrophiles covalently bind to MPO, resulting in an immunogen. Uetrecht's group has shown, through the use of an anti-PA antibody, that PA itself became bound to MPO after metabolism by MPO/$H_2O_2$. The neutrophils from a patient undergoing PA therapy exhibited a 58 kDa protein that was reactive towards anti-PA (63). This protein is believed to be covalently bound to PA through an electrophilic metabolite of PA (e.g., *N*-nitroso-PA, *N*-chloro-PA), or possibly via a free radical metabolite. It would be of great interest to identify this protein, which could possibly be MPO. Although we have determined that MPO forms a free radical in HL-60 cells, it is certainly not the only target for free radical formation (Fig. 6A) and may or may not be the most relevant target in relation to agranulocytosis. In this regard, a recent study in dogs treated with sulfonamide, an aromatic amine drug, showed that anti-MPO and anti-cathepsin G antibodies were detected in sera (64).

In summary, we have shown that PA, a drug associated with agranulocytosis, induced the formation of an MPO free radical in a pure enzymatic system and in HL-60 cells. These findings warrant further study into the toxicological relevance of an MPO free radical *in vivo* and the possible role it may play in the pathogenesis of PA-induced agranulocytosis. Future studies will be conducted with a larger set of MPO substrates to ascertain whether or not there is a correlation between drug-induced MPO protein free radical formation and agranulocytosis.

## Acknowledgements

We would like to acknowledge Dr. Colin Chignell for use of his cell culture facility and thank Dr. Andres G. Cisneros for his help with molecular orbital calculations. Also, we thank Ms. Jean Corbett for the purification of DMPO and Dr. Ann Motten and Ms. Mary Mason for their careful review of the manuscript. We thank the reviewer for suggesting the experiment with dehydroascorbate. This research was supported by the Intramural Research Program of the NIH, and NIH/NIEHS.

## Abbreviations

PA, procainamide; NAPA, *N*-acetylprocainamide; MPO, myeloperoxidase; ESR, electron spin resonance; DTPA, diethylenetriaminepentaacetic acid; MNP, 2-methyl-2-nitrosopropane; DMPO, 5,5-dimethyl-1-pyrroline *N*-oxide; ABAH, 4-aminobenzoic acid hydrazide.

## References


(1). Prystowsky EN, Benson DW Jr. Fuster V, Hart RG, Kay GN, Myerburg RJ, Naccarelli GV, Wyse DG. Management of patients with atrial fibrillation. A Statement for Healthcare Professionals. From the Subcommittee on Electrocardiography and Electrophysiology, American Heart Association. Circulation 1996;93:1262–1277. [PubMed: 8653857]

(2). Ip J, Uetrecht JP. In vitro and animal models of drug-induced blood dyscrasias. Environ. Toxicol. Pharmacol 2006;21:135–140.

(3). Wintrobe, MM.; Greer, J. Wintrobe's Clinical Hematology. Greer, JP.; Foerster, J.; Lukens, JN.; Rodgers, GM.; Paraskevas, F.; Glader, B., editors. Lippincott Williams & Wilkins; Philadelphia: 2003.

(4). Freed JS, Reiner MA. Septic complications of procainamide-induced agranulocytosis: report of two cases. Mt. Sinai J. Med 1988;55:194–197. [PubMed: 3290673]

(5). Dorr VJ, Cook J. Agranulocytosis and near fatal sepsis due to 'Mexican aspirin' (dipyrone). South. Med. J 1996;89:612–614. [PubMed: 8638202]

(6). Young JA, Newcomer LN, Keller AM. Aminoglutethimide-induced bone marrow injury. Report of a case and review of the literature. Cancer 1984;54:1731–1733. [PubMed: 6478412]

(7). van der Klauw MM, Wilson JHP, Stricker BHC. Drug-associated agranulocytosis: 20 years of reporting in The Netherlands (1974-1994). Am. J. Hematol 1998;57:206–211. [PubMed: 9495370]

(8). Ellrodt AG, Murata GH, Riedinger MS, Stewart ME, Mochizuki C, Gray R. Severe neutropenia associated with sustained-release procainamide. Ann. Intern. Med 1984;100:197–201. [PubMed: 6691661]

(9). Kaufman DW, Kelly JP, Jurgelon JM, Anderson T, Issaragrisil S, Wiholm BE, Young NS, Leaverton P, Levy M, Shapiro S. Drugs in the aetiology of agranulocytosis and aplastic anaemia. Eur. J. Haematol. Suppl 1996;57:23–30. [PubMed: 8987237]

(10). Saito, Y. NORD Guide to Rare Disorders. Lippincott Williams & Wilkins; Philadelphia: 2003. Acquired Agranulocytosis; p. 361-362.

(11). Uetrecht JP. The role of leukocyte-generated reactive metabolites in the pathogenesis of idiosyncratic drug reactions. Drug. Metab. Rev 1992;24:299–366. [PubMed: 1628536]

(12). Gill HJ, Hough SJ, Naisbitt DJ, Maggs JL, Kitteringham NR, Pirmohamed M, Park BK. The relationship between the disposition and immunogenicity of sulfamethoxazole in the rat. J. Pharmacol. Exp. Ther 1997;282:795–801. [PubMed: 9262343]

(13). Brown KE, Brunt EM, Heinecke JW. Immunohistochemical detection of myeloperoxidase and its oxidation products in Kupffer cells of human liver. Am. J. Pathol 2001;159:2081–2088. [PubMed: 11733358]

(14). Dunford, HB. Heme peroxidases. John Wiley; New York: 1999.

(15). O'Brien PJ. Peroxidases. Chem. Biol. Interact 2000;129:113–139. [PubMed: 11154738]

(16). Nauseef WM. Myeloperoxidase biosynthesis by a human promyelocytic leukemia cell line: insight into myeloperoxidase deficiency. Blood 1986;67:865–872. [PubMed: 3006833]

(17). Andrews PC, Krinsky NI. The reductive cleavage of myeloperoxidase in half, producing enzymically active hemi-myeloperoxidase. J. Biol. Chem 1981;256:4211–4218. [PubMed: 6260790]

(18). Hansson M, Olsson I, Nauseef WM. Biosynthesis, processing, and sorting of human myeloperoxidase. Arch. Biochem. Biophys 2006;445:214–224. [PubMed: 16183032]

(19). Kettle AJ, Winterbourn CC. Mechanism of inhibition of myeloperoxidase by anti-inflammatory drugs. Biochem. Pharmacol 1991;41:1485–1492. [PubMed: 1850278]

(20). Galati G, Tafazoli S, Sabzevari O, Chan TS, O'Brien PJ. Idiosyncratic NSAID drug induced oxidative stress. Chem. Biol. Interact 2002;142:25–41. [PubMed: 12399153]

(21). Siraki AG, Bonini MG, Jiang J, Ehrenshaft M, Mason RP. Aminoglutethimide-induced protein free radical formation on myeloperoxidase: a potential mechanism of agranulocytosis. Chem. Res. Toxicol 2007;20:1038–1045. [PubMed: 17602675]

(22). Dolman KM, Gans ROB, Vervaat TJ, Zevenbergen G, Maingay D, Nikkels RE, Donker AJM, von dem Borne AEGK, Goldschmeding R. Vasculitis and antineutrophil cytoplasmic autoantibodies associated with propylthiouracil therapy. Lancet 1993;342:651–652. [PubMed: 8103148]

(23). Waldhauser L, Uetrecht J. Antibodies to myeloperoxidase in propylthiouracil-induced autoimmune disease in the cat. Toxicology 1996;114:155–162. [PubMed: 8947614]

(24). Hsuanyu Y, Dunford HB. Oxidation of clozapine and ascorbate by myeloperoxidase. Arch. Biochem. Biophys 1999;368:413–420. [PubMed: 10441395]

(25). Beers RF Jr. Sizer IW. A spectrophotometric method for measuring the breakdown of hydrogen peroxide by catalase. J. Biol. Chem 1952;195:133–140. [PubMed: 14938361]

(26). Bonini MG, Siraki AG, Bhattacharjee S, Mason RP. Glutathione-induced radical formation on lactoperoxidase does not correlate with the enzyme's peroxidase activity. Free Radic. Biol. Med 2007;42:985–992. [PubMed: 17349926]

(27). Lagercrantz C. Spin trapping of some short-lived radicals by the nitroxide method. J. Phys. Chem 1971;75:3466–3475.

(28). Ramirez DC, Mejiba S. E. Gomez, Mason RP. Mechanism of hydrogen peroxide-induced Cu,Zn-superoxide dismutase-centered radical formation as explored by immuno-spin trapping: the role of copper- and carbonate radical anion-mediated oxidations. Free Radic. Biol. Med 2005;38:201–214. [PubMed: 15607903]

(29). Hope HR, Remsen EE, Lewis C Jr. Heuvelman DM, Walker MC, Jennings M, Connolly DT. Large-scale purification of myeloperoxidase from HL60 promyelocytic cells: characterization and comparison to human neutrophil myeloperoxidase. Protein Expr. Purif 2000;18:269–276. [PubMed: 10733879]

(30). Detweiler CD, Deterding LJ, Tomer KB, Chignell CF, Germolec D, Mason RP. Immunological identification of the heart myoglobin radical formed by hydrogen peroxide. Free Radic. Biol. Med 2002;33:364–349. [PubMed: 12126758]

(31). Marquez LA, Huang JT, Dunford HB. Spectral and kinetic studies on the formation of myeloperoxidase compounds I and II: roles of hydrogen peroxide and superoxide. Biochemistry 1994;33:1447–1454. [PubMed: 8312264]

(32). Motten AG, Chignell CF. Spectroscopic studies of cutaneous photosensitizing agents--III. Spin trapping of photolysis products from sulfanilamide analogs. Photochem. Photobiol 1983;37:17–26. [PubMed: 6300940]

(33). Chignell CF, Kalyanaraman B, Mason RP, Sik RH. Spectroscopic studies of cutaneous photosensitizing agents-I. Spin trapping of photolysis products from sulfanilamide, 4-aminobenzoic acid and related compounds. Photochem. Photobiol 1980;32:563–571.

(34). Gasanov RG, Freidlina RK. ESR study of the interaction of mononuclear and binuclear metal carbonyls with silicon hydrides and the use of these systems to generate α-chlorine-containing radicals. Russ. Chem. Bull 1981;30:980–984.

(35). Torssell K. Investigation of radical intermediates in organic reactions by use of nitroso compounds as scavengers: the nitroxide method. Tetrahedron 1970;26:2759–2773.

(36). Kadiiska MB, De Costa KS, Mason RP, Mathews JM. Reduction of 1,3-diphenyl-1-triazene by rat hepatic microsomes, by cecal microflora, and in rats generates the phenyl radical metabolite: an ESR spin-trapping investigation. Chem. Res. Toxicol 2000;13:1082–1086. [PubMed: 11087429]

(37). Sinha BK. Enzymatic activation of hydrazine derivatives. A spin-trapping study. J. Biol. Chem 1983;258:796–801. [PubMed: 6296081]

(38). Guaiquil VH, Farber CM, Golde DW, Vera JC. Efficient transport and accumulation of vitamin C in HL-60 cells depleted of glutathione. J. Biol. Chem 1997;272:9915–9921. [PubMed: 9092530]

(39). Davies MJ, Hawkins CL. EPR spin trapping of protein radicals. Free Radic. Biol. Med 2004;36:1072–1086. [PubMed: 15082061]

(40). Uetrecht J, Zahid N, Rubin R. Metabolism of procainamide to a hydroxylamine by human neutrophils and mononuclear leukocytes. Chem. Res. Toxicol 1988;1:74–78. [PubMed: 2979715]

(41). Uetrecht JP, Zahid N. N-Chlorination and oxidation of procainamide by myeloperoxidase: toxicological implications. Chem. Res. Toxicol 1991;4:218–222. [PubMed: 1664258]

(42). Huie RE, Neta P. Kinetics of one-electron transfer reactions involving $ClO_2$ and $NO_2$. J. Phys. Chem 1986;90:1193–1198.

(43). Ator MA, David SK, de Montellano P. R. Ortiz. Stabilized isoporphyrin intermediates in the inactivation of horseradish peroxidase by alkylhydrazines. J. Biol. Chem 1989;264:9250–9257. [PubMed: 2722829]

(44). Huang L, Colas C, de Montellano P. R. Ortiz. Oxidation of carboxylic acids by horseradish peroxidase results in prosthetic heme modification and inactivation. J. Am. Chem. Soc 2004;126:12865–12873. [PubMed: 15469283]

(45). Kettle AJ, Gedye CA, Winterbourn CC. Mechanism of inactivation of myeloperoxidase by 4-aminobenzoic acid hydrazide. Biochem. J 1997;321:503–508. [PubMed: 9020887]

(46). de Montellano, P. R. Ortiz; David, SK.; Ator, MA.; Tew, D. Mechanism-based inactivation of horseradish peroxidase by sodium azide. Formation of meso-azidoprotoporphyrin IX. Biochemistry 1988;27:5470–5476. [PubMed: 3179265]

(47). Siraki AG, O'Brien PJ. Prooxidant activity of free radicals derived from phenol-containing neurotransmitters. Toxicology 2002;177:81–90. [PubMed: 12126797]

(48). Rubin RL, Curnutte JT. Metabolism of procainamide to the cytotoxic hydroxylamine by neutrophils activated in vitro. J. Clin. Invest 1989;83:1336–1343. [PubMed: 2539397]

(49). Josephy PD, Eling TE, Mason RP. An electron spin resonance study of the activation of benzidine by peroxidases. Molecular pharmacology 1983;23:766–770. [PubMed: 6306434]

(50). Zhan C-G, Nichols JA, Dixon DA. Ionization potential, electron affinity, electronegativity, hardness, and electron excitation energy: Molecular properties from density functional theory orbital energies. J. Phys. Chem. A 2003;107:4184–4195.

(51). Parker VD. Energetics of electrode reactions II. The relationship between redox potentials, ionization potentials, electron affinities, and solvation energies of aromatic hydrocarbons. J. Am. Chem. Soc 1976;98:98–103.

(52). Cavalieri EL, Rogan EG, Roth RW, Saugier RK, Hakam A. The relationship between ionization potential and horseradish peroxidase/hydrogen peroxide-catalyzed binding of aromatic hydrocarbons to DNA. Chem. Biol. Interact 1983;47:87–109. [PubMed: 6640787]

(53). Halliwell B. Antioxidants in human health and disease. Annu. Rev. Nutr 1996;16:33–50. [PubMed: 8839918]

(54). Halliwell B. Dietary polyphenols: good, bad, or indifferent for your health? Cardiovasc. Res 2007;73:341–347. [PubMed: 17141749]

(55). Reidenberg MM. Aromatic amines and the pathogenesis of lupus erythematosus. Am. J. Med 1983;75:1037–1042. [PubMed: 6196968]

(56). Perry HM Jr. Late toxicity to hydralazine resembling systemic lupus erythematosus or rheumatoid arthritis. Am. J. Med 1973;54:58–72. [PubMed: 4581906]

(57). Starkebaum G, Kenyon CM, Simrell CR, Creamer JI, Rubin RL. Procainamide-induced agranulocytosis differs serologically and clinically from procainamide-induced lupus. Clin. Immunol. Immunopathol 1996;78:112–119. [PubMed: 8625553]

(58). Swain SD, Rohn TT, Quinn MT. Neutrophil priming in host defense: role of oxidants as priming agents. Antioxid. Redox. Signal 2002;4:69–83. [PubMed: 11970845]

(59). Arnljots K, Olsson I. Myeloperoxidase precursors incorporate heme. J. Biol. Chem 1987;262:10430–10433. [PubMed: 3038881]

(60). Koeffler HP, Ranyard J, Pertcheck M. Myeloperoxidase: its structure and expression during myeloid differentiation. Blood 1985;65:484–491. [PubMed: 2981591]

(61). Azocar J. Anti-myeloid-cell antibody in procainamide-induced agranulocytosis. Lancet 1984;1:1069–1070. [PubMed: 6143992]

(62). Baker EJ, Gerard DA, Bamberger EG, Lozzio CB, Ichiki AT. HL-60 cell growth-conditioned medium is an effective inducer of myeloperoxidase expression in K-562 human leukemia cells. Leuk. Res 2002;26:1017–1025. [PubMed: 12363471]

(63). Gardner I, Popovic M, Zahid N, Uetrecht JP. A comparison of the covalent binding of clozapine, procainamide, and vesnarinone to human neutrophils in vitro and rat tissues in vitro and in vivo. Chem. Res. Toxicol 2005;18:1384–1394. [PubMed: 16167830]

(64). Lavergne SN, Drescher NJ, Trepanier LA. Anti-myeloperoxidase and anti-cathepsin G antibodies in sulphonamide hypersensitivity. Clin. Exp. Allergy 2008;38:199–207. [PubMed: 17976219]

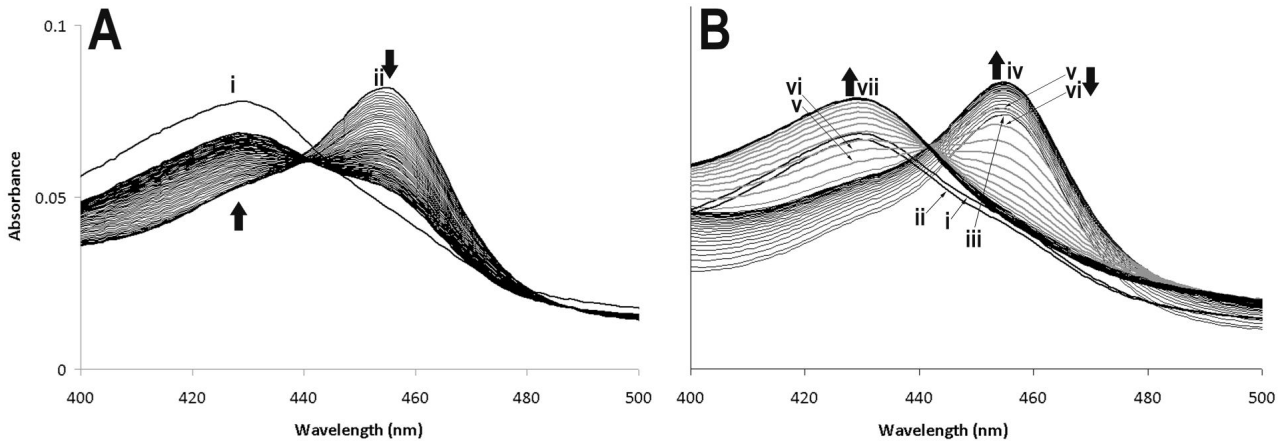


**Figure 1. PA induces MPO Compound II accumulation**

The MPO Soret region was recorded once every minute in the absence (A) or presence (B) of PA for 60 minutes. In (A), resting MPO (500 nM) was recorded first (*i*), followed by the addition of 80 μM $H_2O_2$ (*ii*). In (B), resting MPO (500 nM) was recorded first (*i*), followed by the addition of 20 μM PA (*ii*), and finally 80 μM $H_2O_2$ (*iii*). MPO compound II accumulation continued for 27 minutes (iv). Thereafter, compound II was reduced (v — 28 min, vi - 29 min), and the resting enzyme was reformed at 38 min (vii).

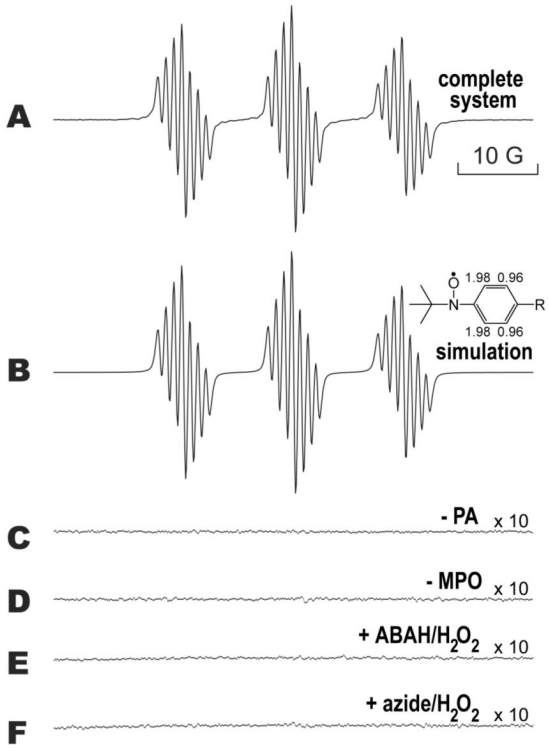


**Figure 2. ESR of the PA free radical metabolite formed by MPO/$H_2O_2$ using the spin trap MNP**

In spectrum A, PA (5 mM) and MNP (10 mM) were added to 200 μL of a solution of 750 nM MPO. The reaction was performed in 0.1 M phosphate buffer (Chelex-100 treated), pH 7.4, and was initiated by the addition of 1 mM $H_2O_2$. ESR settings are described in Experimental Procedures, with the following changes: modulation amplitude = 0.4 G and receiver gain = $2\times10^5$. In B, a computer-simulated spectrum is shown that closely matched the actual experimental spectrum in A (r = 0.98). The hyperfine splitting constants were $a^H_{(2,6)}$ = 0.970 G, $a^H_{(3,5)}$ = 1.98 G and $a^N$ = 13.8 G. In C, the resulting spectrum when PA was omitted from the reaction is shown, and D shows the spectrum when MPO was omitted. In E, MPO was incubated for 30 minutes at 37 °C with 250 μM ABAH and 250 μM $H_2O_2$ before the addition of PA, MNP, and 1 mM $H_2O_2$. The same was performed in F, except that 500 μM azide and 500 μM $H_2O_2$ were preincubated. Incubation of MPO with 500 μM $H_2O_2$ for 30 minutes resulted in no inhibition of activity (data not shown). The scale of spectra C-F were increased 10-fold to show that the spectra had minimal noise and no signal.

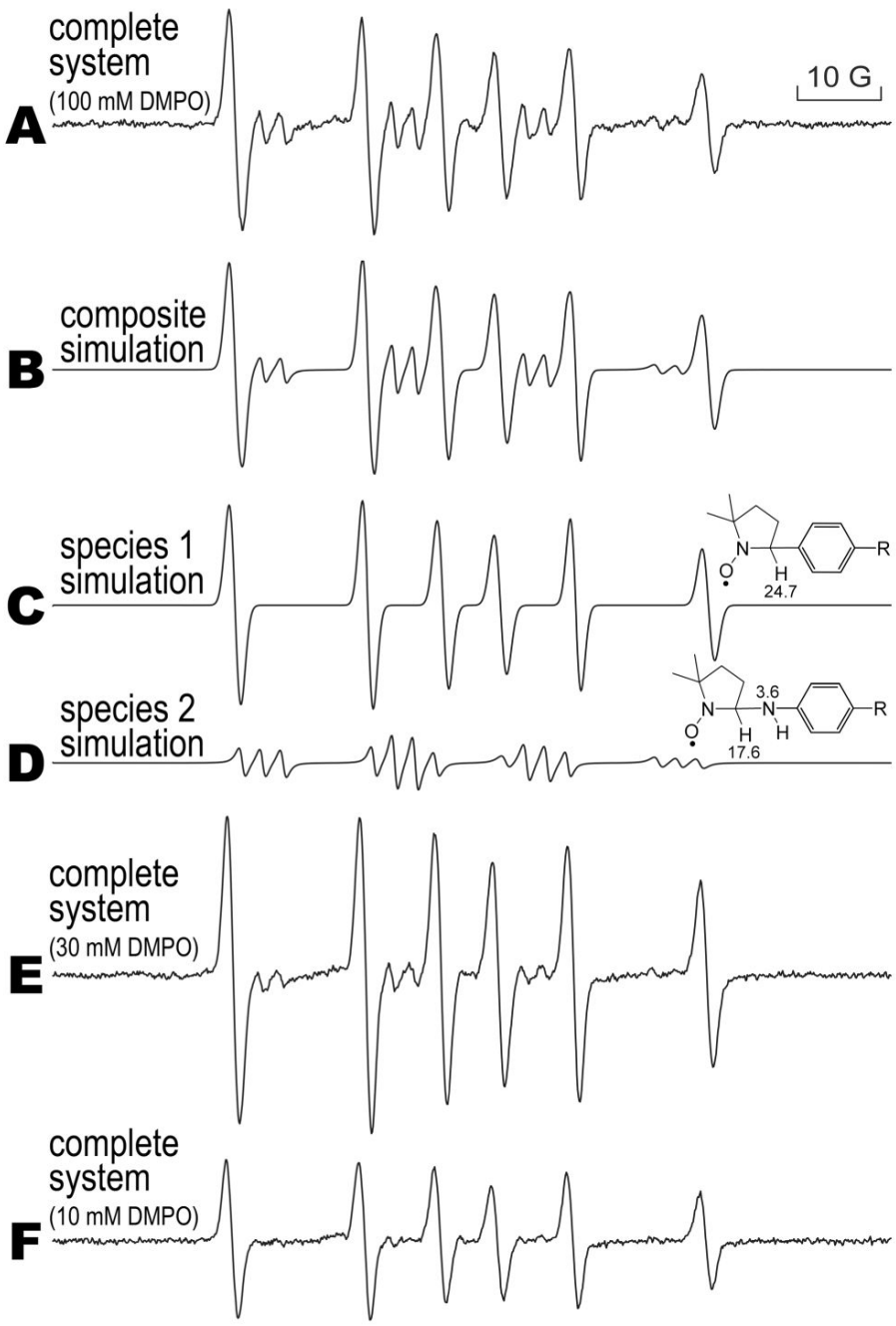


**Figure 3. ESR spin trapping of PA free radical metabolites formed by MPO/$H_2O_2$ using DMPO**

The reaction was performed in 0.1 M phosphate buffer (Chelex-100 treated), pH 7.4. The spectrum in A (complete system) was produced when 5 mM PA, 100 mM DMPO, 750 nM MPO, and 1 mM $H_2O_2$ were mixed. This spectrum contained two species (two different metabolites) for which the composite simulation is shown in B. In C, the first species was simulated ($a^N$ = 15.8 G and $a^H$ = 24.8 G), and in D the second species was simulated ($a^N_{(nitroxide)}$ = 15.7 G, $a^N$ = 2.45 G and $a^H$ = 18.2 G). When 30 mM DMPO was used (E), species 1 became smaller, and became undetectable in F where 10 mM DMPO was used.

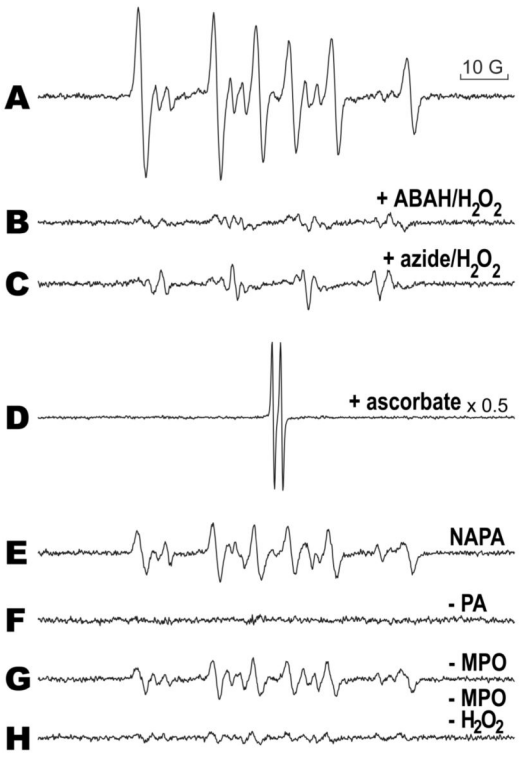


**Figure 4. MPO inhibitors, ascorbate, and NAPA attenuate free radical metabolite detection**

The spectrum in A (complete system) represents the same conditions as in Fig. 3A. In B, 250 μM ABAH with 250 μM $H_2O_2$ was incubated with MPO for 30 minutes at 37 °C before the addition of PA, DMPO, and $H_2O_2$. The same was performed in C, except that 500 μM azide and 500 μM $H_2O_2$ were incubated with MPO. In D, 10 mM ascorbate was included in the reaction (the spectrum intensity was scaled down by 0.5 because of the intense ascorbyl radical), and in E, PA was replaced with NAPA, resulting in a less intense signal than in A. The absence of PA, MPO, or MPO/$H_2O_2$, is shown in F, G, and H, respectively; all show diminished or no signal compared to A.

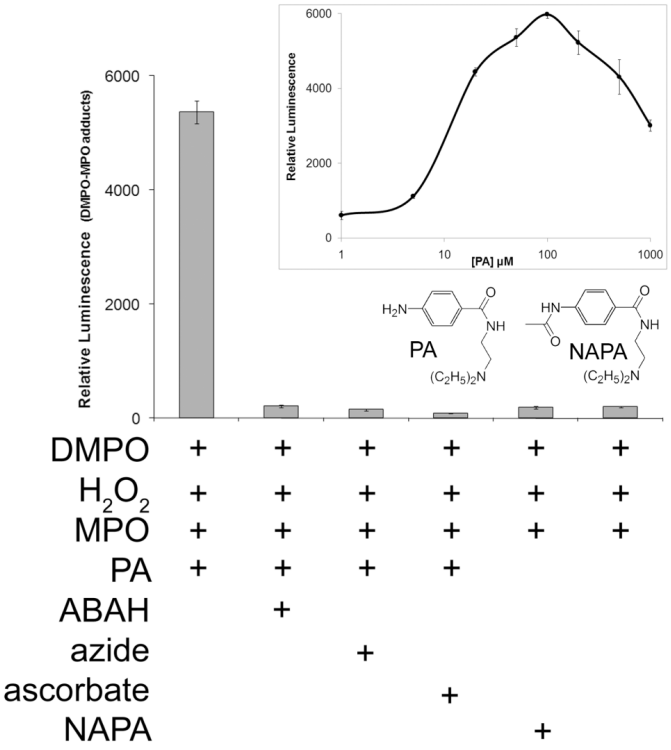


**Figure 5. ELISA of MPO-DMPO formation catalyzed by PA metabolism by MPO/$H_2O_2$**

Reactions were performed in Chelex-100 treated 0.1 M phosphate buffer, pH 7.4. The incubation of DMPO (100 mM), $H_2O_2$ (100 μM), PA (100 μM), and MPO (50 nM, added last) resulted in anti-DMPO binding. The presence of ABAH (1 mM), azide (1 mM), or ascorbate (1 mM) attenuated the signal with similar efficacy. The absence of PA or its substitution with 100 μM NAPA resulted in greatly decreased antibody recognition. MPO-DMPO detection was carried out using polyclonal anti-DMPO as described in Experimental Procedures. Error bars represent ±SD of three wells.

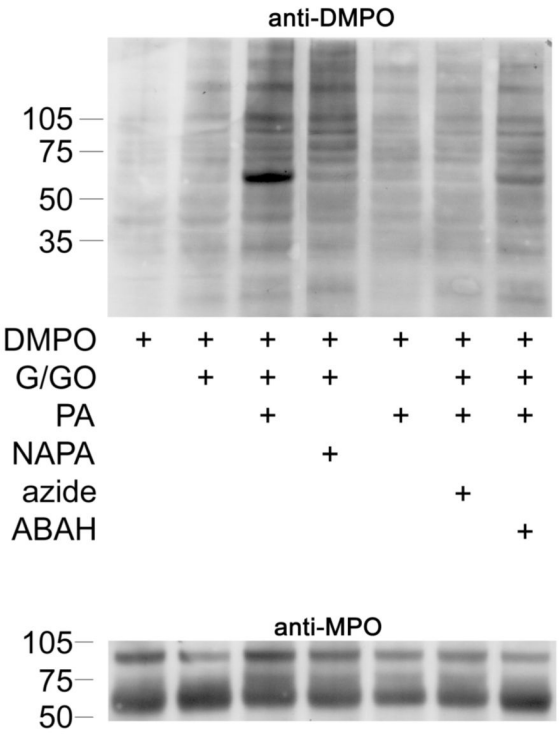


**Figure 6A. Western blot (anti-DMPO) of HL-60 cells after incubation with PA and inhibitors**

HL-60 cells ($2 \times 10^6$/mL, 2 mL) were preincubated with DMPO (50 mM) for 10 minutes before the addition of 1 mM PA. Azide (1 mM) and ABAH (1 mM) were preincubated for 30 minutes with 100 μM $H_2O_2$ and washed once with fresh media before the addition of DMPO. The reaction was initiated with 5 mM glucose / 50 mU/mL glucose oxidase (G/GO), which was added last. The reaction was shaken for 5 minutes on a plate stirrer every 30 minutes and was maintained in a water-jacketed incubator at 37 °C, 5 % $CO_2$ for 4 hours. 10 μg/lane were loaded for anti-DMPO detection, and 1 μg/lane was loaded for anti-MPO.

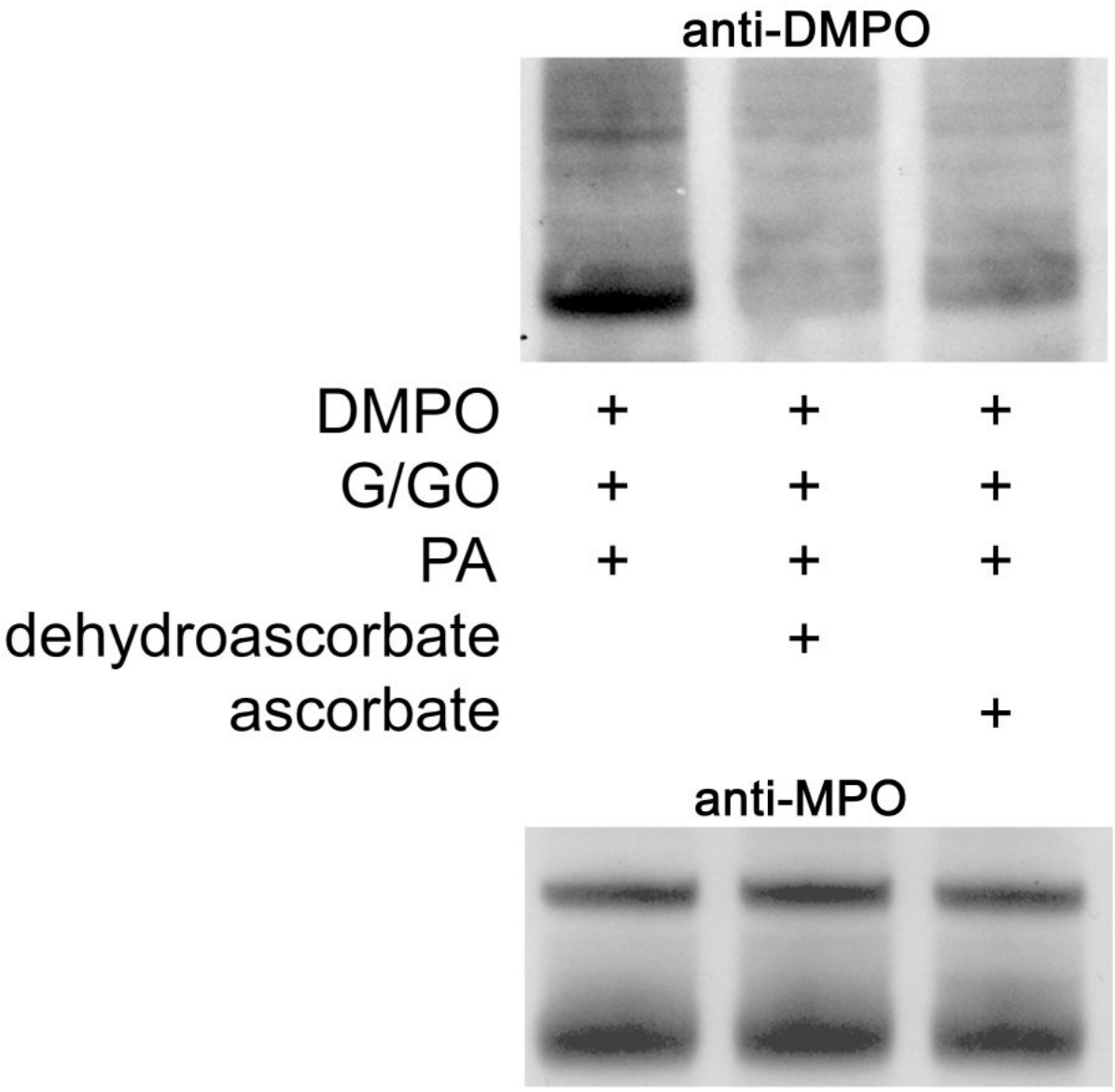


**Figure 6B. Dehydroascorbate and ascorbate attenuate PA-induced anti-DMPO detection**
The effect of the addition of dehydroascorbate (5 mM) and sodium ascorbate (5 mM) 30 minutes before adding PA on protein free radical formation are shown. Dehydroascorbate appeared qualitatively more effective than ascorbate in attenuating PA-induced anti-DMPO detection.

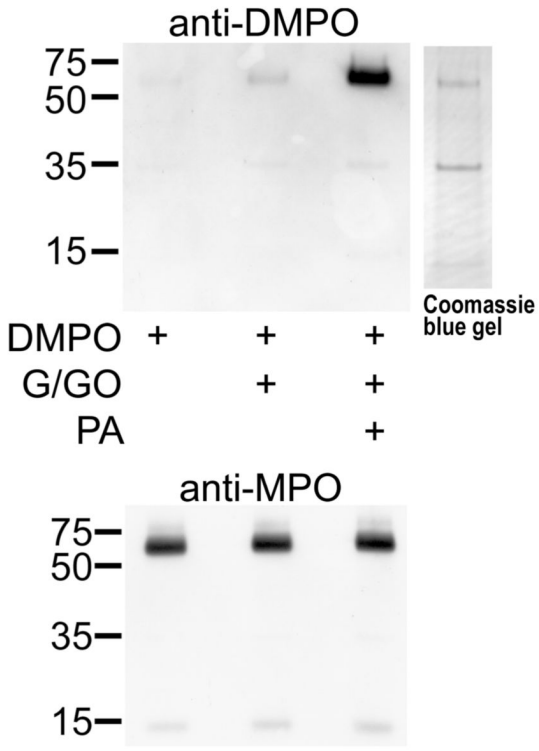


**Figure 6C. Affinity purified with concanavalin A MPO from HL-60 cells is bound to DMPO when incubated with PA**

HL-60 cell incubations were carried out as in 4A, except with 5 mL of cells in order to obtain sufficient MPO for affinity purification. In the anti-DMPO Western blot, 20 μg of protein were loaded into each lane. The corresponding Commassie blue-stained gel is shown adjacent to the anti-DMPO membrane. After exposure to X-ray film, the membrane was stripped and reprobed with anti-MPO.

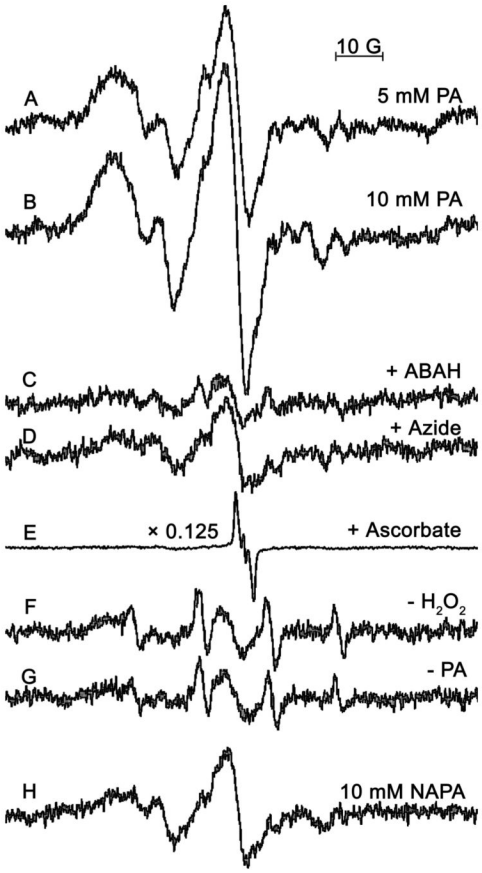


**Figure 7. ESR spectra showing the detection of a protein free radical from HL-60 cell lysates treated with PA and $H_2O_2$**

Cell lysates were obtained as described in Experimental Procedures. Reactions contained 7 mg/ml of dialyzed lysate, 1 mM MNP (spin trap), variable concentrations of PA, and 1 mM $H_2O_2$ (added last). Reactions were heated at 37 °C and mixed for 2 minutes before spectra were recorded. Spectra A and B show a PA dose-dependent increase in protein free radical intensity. 10 mM PA was used for the remaining experiments. The spectrum was attenuated in the presence of 1 mM ABAH (C), 50 mM azide (D), 10 mM ascorbate (E), and when either $H_2O_2$ (F) or PA (G) was omitted from the reaction. Ascorbate produced an intense ascorbyl radical. When 10 mM NAPA (H) was substituted for PA, a less intense protein radical spectrum was recorded. ESR settings are described in Experimental Procedures.

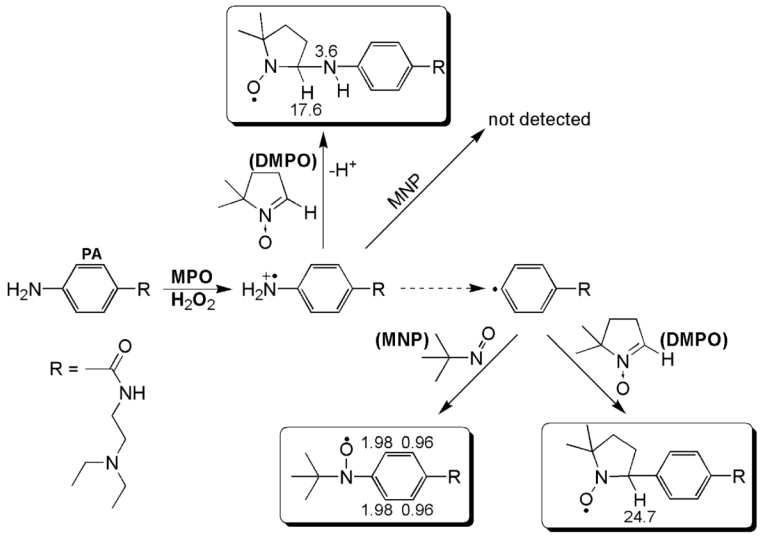


**Scheme 1. PA free radical metabolites formed and trapped by DMPO and MNP**

The first metabolite of PA produced by MPO/$H_2O_2$ was an *N*-centered cation radical, which was trapped with DMPO. MNP may also trap this radical metabolite, but the adduct may be unstable since it was not detected. The dashed arrow indicates that the mechanism of phenyl radical formation is not currently known. The phenyl radical was trapped with MNP and/or DMPO. Each spin adduct shows their associated coupling constants.

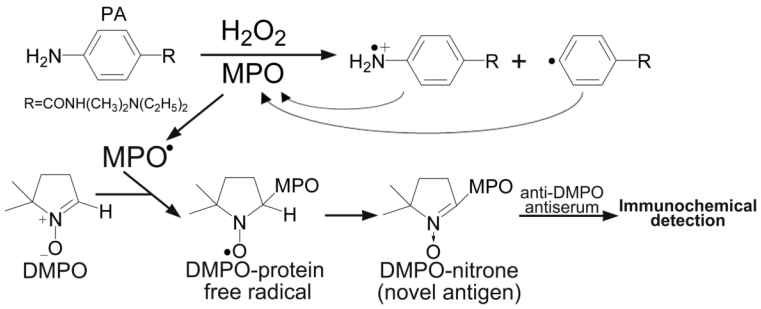


**Scheme 2. Postulated mechanisms of PA reactive free radical metabolite induced modification of proteins, especially MPO**

PA metabolism by MPO results in cation radical formation and in phenyl radical formation, where one or both of these species attacks MPO resulting in MPO protein free radical formation. The latter can be trapped by DMPO, resulting in a spin adduct that we detect by immunological methods.

## Table 1

Ionization Potentials of PA and NAPA.

| | Ionization Potential (eV)* | |
|---|---|---|
| | AM1 energy | PM3 energy |
| PA | 8.70 | 8.43 |
| NAPA | 9.05 | 8.97 |

* Values were calculated by the MOPAC v.6 interface in Sybyl 7.3 using AM1 geometry and AM1 and PM3 energy calculations as described in Experimental Procedures.